Department of Pharmaceutical Sciences/Center for Drug Research and Development (CDRD), College of Pharmacy, Howard University, Washington D.C., USA

D-Optimal mixture experimental design for stealth biodegradable crosslinked docetaxel-loaded poly-ε-caprolactone nanoparticles manufactured by dispersion polymerization

O. Ogunwuyi, S. Adesina, E. O. Akala

Received June 28, 2014, accepted September 14, 2014

Prof. Emmanuel O. Akala, Department of Pharmaceutical Sciences/Center for Drug Research and Development (CDRD), College of Pharmacy, Howard University, 2300 Fourth Street N.W., Washington D.C. 20059, USA
eakala@howard.edu

Pharmazie 70: 165–176 (2015) *doi: 10.1691/ph.2015.4100*

We report here our efforts on the development of stealth biodegradable crosslinked poly-ε-caprolactone nanoparticles by free radical dispersion polymerization suitable for the delivery of bioactive agents. The uniqueness of the dispersion polymerization technique is that it is surfactant free, thereby obviating the problems known to be associated with the use of surfactants in the fabrication of nanoparticles for biomedical applications. Aided by a statistical software for experimental design and analysis, we used D-optimal mixture statistical experimental design to generate thirty batches of nanoparticles prepared by varying the proportion of the components (poly-ε-caprolactone macromonomer, crosslinker, initiators and stabilizer) in acetone/water system. Morphology of the nanoparticles was examined using scanning electron microscopy (SEM). Particle size and zeta potential were measured by dynamic light scattering (DLS). Scheffe polynomial models were generated to predict particle size (nm) and particle surface zeta potential (mV) as functions of the proportion of the components. Solutions were returned from simultaneous optimization of the response variables for component combinations to (a) minimize nanoparticle size (small nanoparticles are internalized into disease organs easily, avoid reticuloendothelial clearance and lung filtration) and (b) maximization of the negative zeta potential values, as it is known that, following injection into the blood stream, nanoparticles with a positive zeta potential pose a threat of causing transient embolism and rapid clearance compared to negatively charged particles. *In vitro* availability isotherms show that the nanoparticles sustained the release of docetaxel for 72 to 120 hours depending on the formulation. The data show that nanotechnology platforms for controlled delivery of bioactive agents can be developed based on the nanoparticles.

1. Introduction

Recent advances in the field of nanotechnology have made nanoparticles very promising in the discovery and delivery of bioactive agents as well as in diagnostics. The evolution of nanoparticles for biomedical applications has moved from the first generation nanoparticles (mainly suitable for liver targeting) through the second generation (stealth nanoparticles for long blood circulation and passive targeting) to the third generation nanoparticles with molecular recognition (Akala 2010; Hillareau and Couvreur 2006). The fourth generation has been dubbed theranostics: multifunctional nanoscale devices which allow for a combination of diagnostic agent with a therapeutic agent and even a reporter of therapeutic efficacy in the same nanodevice package (Kelkar and Reineke 2011). Aside from biocompatibility and biodegradability, the physicochemical properties of nanoparticles (size and surface modification, among others) and their interactions with biological systems are important considerations in their design and fabrication. Polymeric nanoparticles can be prepared mainly by two methods: (*i*) dispersion of preformed polymers and (*ii*) polymerization of monomers (i.e., *in situ* polymerization). Polymeric materials often used for the method involving dispersion of preformed polymers include natural macromolecules (biopolymers) and synthetic polymers. Among the natural macromolecules available for the manufacture of nanospheres, proteins such as albumin, gelatin, legumin, or vicilin, as well as polysaccharides like alginate or agarose have been evaluated. Among the numerous synthetic polymers available for the preparation of nanoparticles, the most commonly used are PLA, PLGA, poly(glycolic acid) (PGA), poly(ε-caprolactone) (PCL) and poly(β-hydroxybutyrate) (PHB). Belonging to the family of polyesters, these polymers are known to exhibit adequate biodegradability and biocompatibilty. Under physiological conditions, polyesters are generally degraded by hydrolysis into products which are well tolerated by various tissues. For example, the degradation products from PLA, PGA and PLGA, namely glycolic acid and lactic acid, are physiological substances easily eliminated through the Krebs cycle (Akala 2010). *In situ* polymerization of monomers, including crosslinkers, is another method for the fabrication of nanoparticles. The method allows one-pot synthesis of nanoparticles. It offers the following

advantages. Functionalization of the nanoparticles' surface is easy which is needed either to modify the biodistribution of the nanoparticles for long blood circulation by avoiding capture by the reticuloendothelial system (passive targeting) or to achieve site specific uptake in cells (active targeting) by tethering a ligand to nanoparticle surface that can achieve biorecognition by virtue of the receptors expressed on the surface of cells (e.g. cancer cells) (Adesina et al. 2013; Landfester and Mailander 2013). pH-Sensitive nanoparticles can be designed by incorporating appropriate monomers or crosslinkers which can respond to pH changes in the body (Gillies and Fréchet 2004). It is possible to control or sustain the release of drugs and other substances incorporated in the nanoparticles from the interior by using degradable or hydrolyzable crosslinker (Akala and Oluyomi 2013) or enzymes can be used for specific cleavage: preparation of enzyme responsive nanocapsules with payload-release properties (Landfester and Mailander 2013; Landfester et.al 2010). Other stimuli include light, temperature, and reduction of disulfide crosslinker in a reductive environment in the cell (Oliveira et al. 2011). Theranostic nanoparticles can be easily developed by *in situ* polymerization. A case in point is the molecular and functional imaging of breast cancer receptors using a noninvasive technique. The superparamagnetic iron oxide nanoparticles (SPIONs) can be used as a contrast agent in MRI for identifying micrometastases and for breast cancer prognosis. The targeted contrast agents can be directed to cell surface receptors using affibody molecules. Further, affibody-decorated nanoparticles containing SPIONs will be suitable for MRI monitoring of treatment progression both for big tumors and metastases. Furthermore, image-guided placement or accumulation of the drug- and contrast agent-loaded nanoparticles on the surface of breast tumors followed by internalization is possible (Kramer-Marek et al. 2009 and Reilly 2009). All these advantages of *in situ* polymerization derive from the possibility of simultaneous encapsulation of relevant hydrophobic/hydrophilic drugs, nucleic acids, fluorochromes and, by copolymerization, adding surface functionalities in one batch process without further modifications needed for nanoparticle fabrication by dispersion of preformed polymers. Any attempt to modify the surface of nanoparticles fabricated by dispersion of preformed polymers often results in a substantial loss of encapsulated drugs or other materials.

Among the techniques available for *in situ* polymerization for the fabrication of nanoparticles are emulsion polymerization, microemulsion polymerization, miniemulsion polymerization, dispersion polymerization, and suspension polymerization (Adesina et al. 2013; Akala and Oluyomi 2013; Arshady 1992; Hong et al. 2007; Landfester and Mailander 2013; Landfester et al. 2010; Yin et al. 2002). Our laboratory has focused on surfactant free, free radical dispersion polymerization technique for the fabrication of stealth crosslinked nanoaprticles for biomedical applications (Adesina et al. 2013; Akala and Oluyomi 2013). Dispersion polymerization is a technique in which all reacting monomers are soluble in the solvent medium that is a poor or non-solvent for the polymer being formed. The starting reaction mixture is a clear, single-phase solution; particles are formed by precipitation of growing polymer chains in the presence of a suitable steric stabilizer. Therefore, the solvent medium becomes a dispersion medium (Capek 2000; Leobandung et al. 2003; Song et al. 2006; Han et al. 2009; Horak 1999; Ha et al. 2010). Dispersion polymerization occurs in the presence of a dissolved soluble amphiphilic polymer (or *in situ* formed graft copolymer product) which is adsorbed on the surface of particles where it lowers the surface free energy and functions as a steric stabilizer (Ray and Mandal 1999; Kim et al. 2001; Lee et al. 2004; Kawaguchi and Ito 2005).

We report here our efforts on the development of stealth biodegradable cross-linked poly-ε-caprolactone nanoparticles by dispersion polymerization suitable for the delivery of bioactive agents. We have used previously a free radical dispersion polymerization technique in the fabrication of crosslinked PLA-based stealth polymeric nanoparticles using the macromonomer approach (Adesina et al. 2013). The successful use of polymers of lactic acid and glycolic acid as biodegradable drug delivery systems and as biodegradable sutures led naturally to an evaluation of other aliphatic polyesters, and to the discovery of the degradability of PCL *in vivo* (Schindler et al. 1977). Several studies using copolymers of poly-ε-caprolactone have shown that it is biocompatible. Poly-ε-caprolactone undergoes hydrolytic degradation to give an hydrolysis intermediate which produces 6-hydroxycaproic acid. 6-Hydroxycaproic acid is broken down to acetyl-CoA units *via* β-oxidation (fatty acid metabolism) for further degradation *via* the Krebs cycle. Thus PCL is degradable to products that are physiologically metabolized by the body. Among United States Food and Drug Administration-approved polyesters, PCL possesses unique properties such as higher hydrophobicity and neutral biodegradation end products, which do not disturb the pH balance of the degradation medium (Pitt et al. 1981a; Woodward et al. 1985). Over the years, many types of drug delivery systems, including nanoparticles, have been developed using PCL as polymeric material (Pitt et al. 1981b; Sinha et al. 2004; Sinha and Khosla 1998; Shenoy and Amiji 2005).

2. Investigations, results and discussion

2.1. Synthesis and characterization of methacrylate-terminated poly-ε-caprolactone macromonomer

Polyester macomonomers are linear macromonomers carrying polymerizable functional groups at their chain ends. The end-capping of poly-ε-caprolactone macromonomers can be achieved by polymerizing ε-caprolactone using an initiator (e.g. aluminium isopropoxide) followed by esterification of hydroxyl end group by a suitable compound (e.g. methacrylic acid), which involves a two-step process. Alternatively, ring opening polymerization of ε-caprolactone can be done in the presence of an initiator carrying the required functional group. Consequently, following polymerization, one chain end bears an hydroxyl group while the other is capped with the functional group associated with the initiator (one-step process). In this study, methacrylate end functionalized poly-ε-caprolactone (P(CL-HEMA)) was synthesized by a modified published method using hydroxylethylmethacrylate as the initiator (one-step process as shown in Scheme 1) (Liu et al. 1998; Tortosa et al. 1997).

The FT-IR and ^{1}H NMR spectra of the synthesized macromonomer are consistent with the expected structure (Liu et al. 1998; Tortosa et al. 1997). Analysis of the FT-IR spectrum reveals the presence of a C = C stretch at 1635 cm^{-1} corresponding to the vinyl functional group of 2-HEMA. The ^{1}H NMR spectrum confirms the presence of a C = C bond with olefinic (vinylic) protons at $\delta = 5.6$ ppm and $\delta = 6.1$ ppm. These data confirm the incorporation of HEMA into the macromonomer. The number average molecular weight (M_n) was determined by ^{1}H NMR and GPC; while the weight average molecular weight (M_w) was determined by GPC. Molecular weight and polydispersity index of the synthesized macromonomer were determined by gel permeation chromatography (GPC) using a Waters 2690 GPC system equipped with a Waters 2410 differential refractive index detector (Adesina et al. 2013; Akala et al. 2011). Polystyrene standards were used for cal-

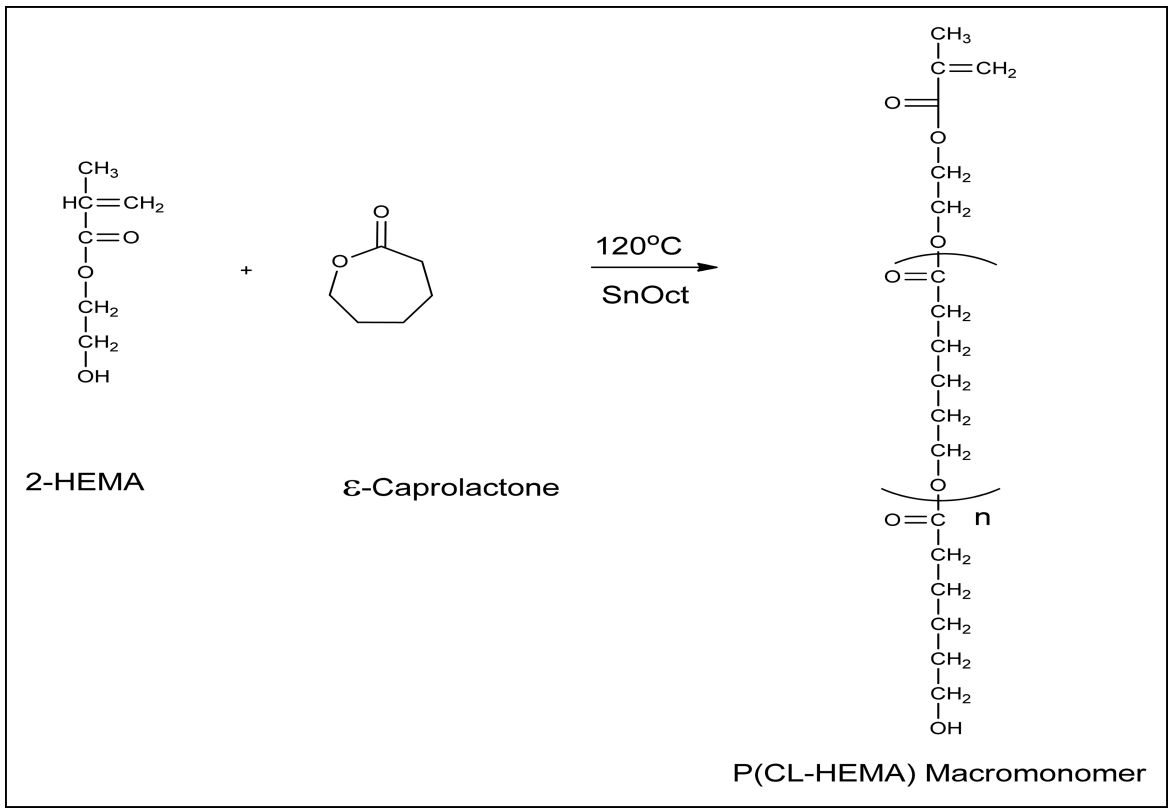

Scheme 1: Ring-opening polymerization scheme for the synthesis of poly(ε -caprolactone) macromonomer.

ibration and tetrahydrofuran was used as mobile phase. The results of poly-ε-caprolactone macromonomer compositions are shown in Table 1. GPC also revealed a single prominent peak.

It was shown that the molecular weight of poly-ε-caprolactone macromonomer is controllable on the basis of the monomer to initiator molar ratio (Dubois et al. 1991). Further, it has been indicated that with increasing caprolactone/HEMA molar ratio (with decreasing HEMA concentration), the molecular weight of macromonomer obtained increases. Moreover, the higher the stannous octanoate concentration, the greater the number of activated centers, which results in lower molecular weight polymers when all monomers have been consumed (Liu et al. 1998). Consequently, we decided to vary the caprolactone/HEMA molar ratio as shown in Table 1. Data show that the molecular weight of poly- ε-caprolactone-HEMA is predictable on the basis of monomer to initiator (HEMA) molar ratio. Increase in the amount of HEMA resulted in a concomitant decrease in the molecular weight of the end-functionlaized macromonomer. The number average molecular weight (M_n) determined using proton nuclear magnetic resonance decreased from 1916 to 1084, with decrease in the molar ratio of ε-caprolactone: HEMA from 14.96 to 3.75. The data are consistent with those reported by Liu et al. (1998). The poly- ε-caprolactone-HEMA macromonomer with the lowest molecular weight (Table 1) was used for nanoparticle fabrication. The polydispersity index ($PDI_{polymer}$) is 1.08, indicating that the macromonomer has a very narrow molecular weight distribution and is the best value from four different batches shown in Table 1. The discrepancy between the number average molecular weight (M_n)determined by ^{1}H NMR and that determined by GPC using polystyrene standards is common in the literature; it has been ascribed to the use of polystyrene standards for calibration. It is due to differences in the hydrodynamic volume of polystyrene relative to poly- ε-caprolactone-HEMA macromonomer (Adesina et al. 2013; Czelusniak 2007; Ryner et al. 2001).

2.2. Characterization of crosslinker

The FT-IR spectrum of N,O-dimethacryloyl hydroxylamine (MANOHA) shows the presence of C = C stretch at 1626 cm^{-1}.

Table 1: Properties of four different batches of poly-ε-caprolactone-HEMA macromonomer

Molar ratio Caprolactone /HEMA (Feed Composition)	Mn (^{1}H NMR)	Mw (GPC)	*Polydispersity Index ($PDI_{polymer}$)	HEMA (Mole in Feed Composition)	Mol % HEMA (^{1}H NMR) in Macromonomer
14.96	1916	6445	2.13	0.0077	5.51
7.53	1455	3735	1.64	0.0153	7.66
4.98	1360	3294	1.68	0.0231	9.62
3.75	1084	1057	1.08	0.0308	12.35

(ε-caprolactone used for the different batches was held constant: 0.1152 moles)
*$PDI_{polymer}$ = Mw (GPC) / Mn (GPC).

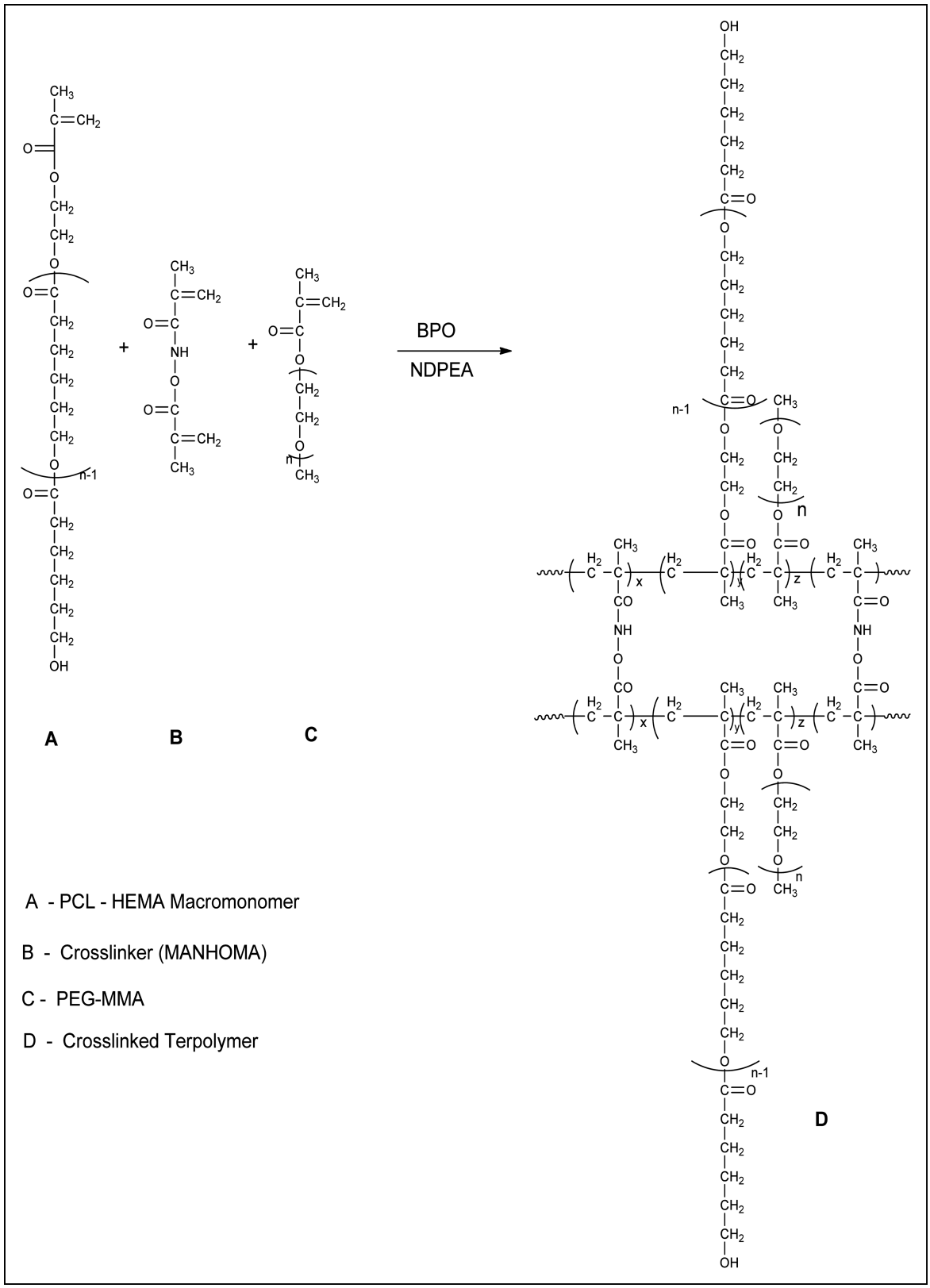

Scheme 2: Synthesis and structure of stealth crosslinked Poly-ε-Caprolactone-HEMA nanoparticle.

The ^{1}H NMR spectrum of N,O-dimethacryloyl hydroxylamine confirms the presence of a divinylic structure with a pair of vinylic protons at about $\delta = 5.8$ ppm and $\delta = 6.3$ ppm and the other at about $\delta = 5.4$ ppm and $\delta = 5.7$ ppm. Melting point analysis is 54 ± 1 °C. All the data obtained are consistent with literature values (Adesina et al. 2013; Akala and Oluyomi 2013; Akala et al. 1998).

2.3. Synthesis and morphological evaluation of blank nanoparticles

The synthesized poly-ε-caprolactone-HEMA macromonomer, crosslinking agent (MANHOMA), benzoyl peroxide/N-phenyldiethanolamine (BPO/NPDEA) redox initiator system and stabilizer (poly(ethylene glycol)*n* monomethyl ether mono methacrylate (PEG-MA), ($n = 1000$): Molecular weight: MW of

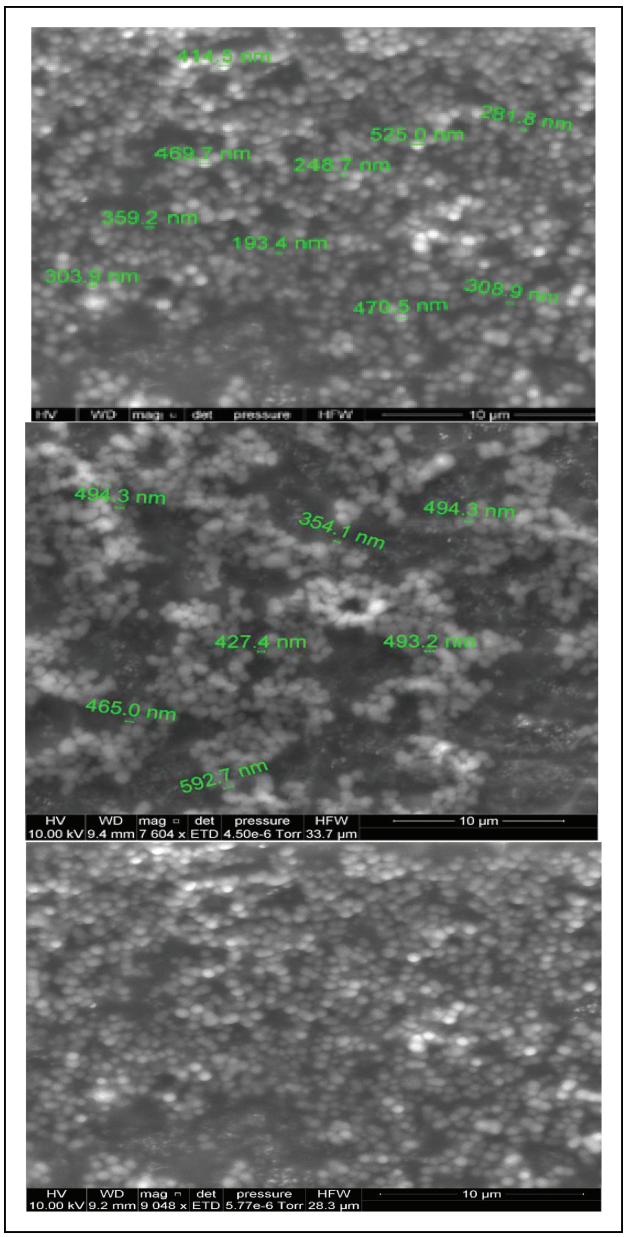

Fig. 1: Typical SEM images of blank stealth poly-ε-caprolactone nanoparticles prepared by *in situ* dispersion polymerization.

PEG Block = 1,000) were used in the synthesis of nanoparticles by the *in situ* dispersion polymerization method (Scheme 2). Synthesis of blank nanoparticle was confirmed by SEM shown in Fig. 1 (representative scanning electron micrographs (SEM). Formation of smooth spherical nanoparticles particles was confirmed.

2.4. Statistical experimental design, particle size and zeta potential analysis

The relatively new concept of quality by design (QbD) in pharmaceutical development, already incorporated into automakers' production principles, involves designing and developing drug formulations and manufacturing processes which ensure predefined drug product specifications. It is believed that product and process understanding is a key element of QbD (Yu 2008). Thus, an important part of QbD is to understand how process and formulation variables affect product characteristics and subsequent optimization of these variables vis-à-vis the final specifications. Statistical design of experiments (DoE) is a well-established method for identifying important parameters in a pharmaceutical

Table 2: Constraints on component concentrations

	Lower limit (mmol)	Upper Limit (mmol)
Crosslinking agent	0.015	0.048
Initiator system[a]	0.298	0.566
Stabilizer	0.209	0.457
Macromonomer	0.166	0.285

[a] Benzoyl peroxide/N-phenyldiethanolamine (1:1)

dosage form design and optimizing the parameters with respect to certain specifications; DoE is a valuable tool to establish in mathematical form the relationships between critical process parameters (CPPs) together with the critical material attributes (CMAs) and critical quality attributes (CQAs). Further, DoE can help identify optimal conditions (Yu et al. 2014). We have indicated earlier that two major approaches to the design of experiments to be able to examine all of the variables simultaneously are factorial and mixture experimental designs (Adesina et al. 2013). When the responses or nanoparticle properties are known to depend on the proportions of the ingredients, mixture designs are preferred. Thus, statistical experimental designs involving mixture methodology is an efficient method for studying products made from the components at various levels (Adesina et al. 2013). We used D-optimal mixture design for experimental design, analysis and optimization. When a formulation is a mixture of various components (proportion of the constituents: macomonomer, crosslinker, PEG (stabilizer) and initiator system) as studied in this work and the levels of the components are constrained, D-optimal mixture design is more useful than a factorial design because it accounts for the dependence of response on proportionality of constituents (Adesina et al. 2013; Shastri et al. 2013; Lewis and Chariot 1991).

This study focuses on a deeper understanding of the fabrication of stealth poly-ε-caprolactone biodegradable nanoparticles by dispersion polymerization. The responses (average particle size (nm) and zeta potential (mV)) are dependent on the proportions of the formulation variables investigated: macromonomer, initiator, stabilizer, and crosslinker. Aided by a statistical software for the design of experiments and analysis of data (Design-Expert®, Stat-Ease Inc.: Wayne and Whitcomb 2014), we examined the effects of the combinations of the components on particle size and zeta potential.

Based on preliminary data, constraints were introduced to the proportions of the components to allow the fabrication of smooth spherical particles within the nanometer size range (Table 2). In D-optimal mixture design, there are restrictions on component proportions such that a lower and an upper limits are specified as reported previously (Adesina et al. 2013; Shastri, et al. 2013; Rajin 2007; Cornell 2002; Lewis and Chariot 1991). Using D-optimal mixture design, with the aid of the statistical software, we varied the components (CMAs: crosslinker, initiator, stabilizer and poly-ε-caprolactone-HEMA macromonomer) to obtain thirty nanoparticle formulations (Table 3). Scheffe polynomial models were generated to predict particle size (nm) and zeta potential (mV) as functions of the composition of the formulations. Simultaneous numerical and graphical optimizations were carried out on the response variables (CQAs): particle size and zeta potential. Particle size and surface zeta potential were determined by dynamic light scattering and are shown in Table 3 below. The values of the zeta potential were negative but were transformed into positive values to facilitate computation; hence the column was labelled negative zeta potential. Dynamic light scattering is a widely used technique for the determination of the particle size of colloidal systems (Adesina et. al. 2013; Cegnar

Table 3: Compositions and responses of D-optimal mixture experimental design for the fabrication of poly-ε-caprolactone stealth nanoparticles

Standard Order	Run order	A: Crosslinking agent (mmol)	B: Initiator system (mmol)	C: Stabilizer (PEG-MMA) (mmol)	D: Macromonomer (mmol)	Response 1 (Particle size: nm)	Response 2 (negative zeta potential: mV)
9	1	0.018	0.358	0.422	0.203	691.5	14.1
11	2	0.038	0.298	0.449	0.215	131.4	36
20	3	0.021	0.480	0.255	0.244	675.9	20.5
19	4	0.027	0.332	0.401	0.240	378.3	31.1
25	5	0.027	0.411	0.311	0.251	328.3	15.3
2	6	0.016	0.499	0.305	0.180	653	29.7
6	7	0.033	0.379	0.397	0.191	148.4	31.7
17	8	0.034	0.502	0.237	0.227	228	28.2
5	9	0.024	0.512	0.279	0.185	235.6	27.4
7	10	0.034	0.438	0.334	0.194	130.8	22
18	11	0.034	0.502	0.237	0.227	224	27.7
14	12	0.019	0.475	0.287	0.219	749	23.1
21	13	0.038	0.407	0.308	0.247	181.3	15.5
27	14	0.045	0.356	0.342	0.257	130.8	36.6
29	15	0.023	0.364	0.350	0.263	687	20
10	16	0.018	0.566	0.213	0.204	635.5	21.4
28	17	0.022	0.451	0.269	0.258	603.6	29.2
23	18	0.032	0.345	0.373	0.249	255.1	25
8	19	0.035	0.556	0.209	0.201	131.6	0.047
30	20	0.037	0.389	0.293	0.281	241	0.0429
24	21	0.027	0.411	0.311	0.251	372.3	17.4
1	22	0.024	0.462	0.347	0.167	242.7	32.4
26	23	0.044	0.442	0.262	0.252	152.6	-0.112
13	24	0.019	0.475	0.287	0.219	550.5	0.0646
4	25	0.024	0.512	0.279	0.185	224	35.8
12	26	0.024	0.366	0.392	0.218	390.7	33.9
16	27	0.020	0.388	0.368	0.224	703	0.0435
22	28	0.038	0.407	0.308	0.247	263.1	0.0421
15	29	0.019	0.304	0.457	0.220	788.6	0.00538
3	30	0.021	0.410	0.384	0.185	325.1	-0.0778

et. al. 2004; Xu et al. 2006). The particle size obtained ranges from 130 nm to 788 nm; while $PDI_{nanoparticle}$ ranges from 0.133 to 0.605. The particle size distribution is given by the polydispersity index ($PDI_{nanoparticle}$). A $PDI_{nanoparticle}$ value of < 0.1 indicates a homogenous monodisperse formulation; while a $PDI_{nanoparticle}$ of > 0.3 indicates polydispersity with variations in particle size (Cegnar et. al. 2004).

Particle size plays an important role in determining the drug release behavior of drug-loaded nanoparticles and the fate of the nanoparticles after *in vivo* administration (Jin et al. 2007; Hongliang et al. 2010). The particles should be small enough to avoid the mechanical spleen or lung filtering effects. Moreover, the cells of the reticuloendothelial system (RES) or mononuclear phagocyte system recognize and rapidly clear nanoparticles from the circulation by phagocytosis and RES uptake has been shown to increase with particle size (Hongliang et al. 2010). Furthermore, it has been reported that smaller particles accumulate more in tumors compared to larger-sized ones by the primary mechanism of passive drug targeting to tumors – the EPR effect (Hongliang et al. 2010). Thus, we directed our efforts at model optimization with emphasis on particle size minimization.

Zeta potential results show predominantly negative values (Table 3). Following injection into the blood stream, nanoparticles with a positive zeta potential pose a threat of causing transient embolism and rapid clearance compared to negatively charged particles. Thus, the pegylated poly-ε-caprolactone-based nanoparticles fabricated by dispersion polymerization are very promising: capable of carrying the drug load to its site of action (Li and Huang 2008). Consequently, we decided to carry out simultaneous numerical optimization on particle size (with emphasis on minimization) and zeta potential (with emphasis on maximization of the negative zeta potential values).

2.5. Data analysis, Scheffe polynomial and optimization

The selection of the best models for modeling the response variables (particle size and zeta potential data) is important since the fitted models will be used to predict the variables following simultaneous numerical optimization (Ulas 2007). With the mixture design, the response determined by any possible component mixtures can be identified by a point in the experimental domain called the design space. When working with three different variables (components), the experimental domain corresponds to an equilateral triangle with the vertices corresponding to the pure components while different points within the design space correspond to a mixture of components (Adesina et al. 2013; Cafaggi et al. 2003). In this work, four components (macromonomer, initiator system, crosslinking agent and stabilizer) were combined to prepare nanoparticles; however, the proportion of the macromonomer was kept constant in all the experiments thereby yielding a triangular experimental domain. Further, as a result of constraints introduced, the region of interest (design space) that allows for the formation of smooth spherical particles is only a fraction of the possible experimental domain (Figs. 2 and 3). Typical particle size and zeta potential data are shown in Figs. 4 and 5.

Logarithmic transformation was carried out before model fitting to particle size data. The quadratic model was found significant

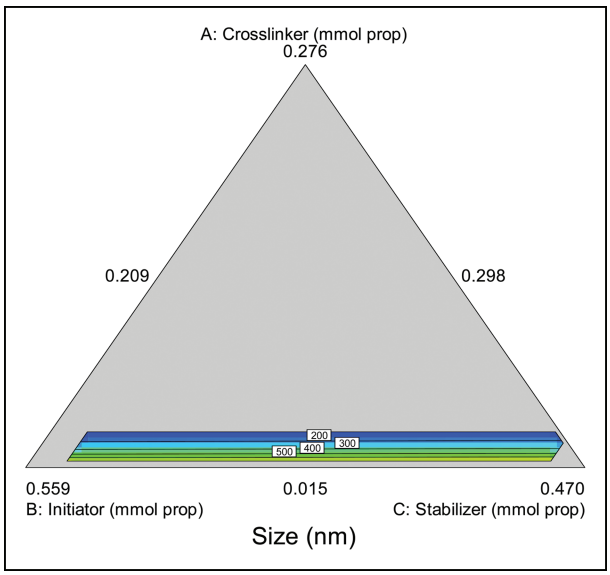

Fig. 2: Model graph showing the design space and variation in particle size as a function of the mixture composition. A = Crosslinking agent; B = Initiators; C = Stabilizer and D = Macromonomer.

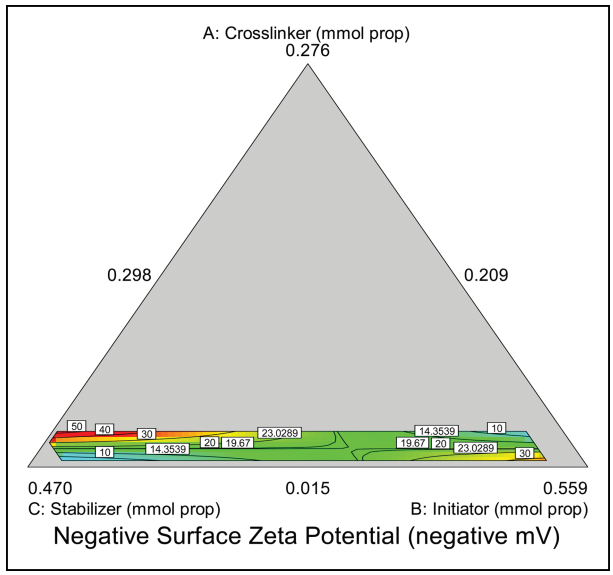

Fig. 3: Model graph showing the design space and variation in zeta potential as a function of the mixture composition. A = Crosslinking agent; B = Initiators; C = Stabilizer and D = Macromonomer.

and was selected. To improve the model, insignificant terms were removed by backward elimination. Analysis of variance (ANOVA) of the selected model and terms (Table 4) reveals that the selected model is significant ($p < 0.0001$). The linear mixture (component linear terms) and the square of A term (crosslinker term) are significant: $p < 0.0001$ and $p = 0.0005$ respectively. Also, "lack of fit" is not significant ($p = 0.6921$). Non-significant lack of fit is good as our desire is for the model to fit. The "Pred R-Squared" of 0.9326 is in reasonable agreement with the "Adj R-Squared" of 0.9455. Adeq Precision measures the signal to noise ratio. A ratio greater than 4 is desirable. The ratio of 27.332 obtained in this work indicates an adequate signal. Consequently, this model can be used to navigate the design space.

The empirical model (Scheffe polynomial) is shown in eq. 1 below:

$$\begin{aligned} \mathrm{Log}_{10}(\mathrm{Size}) = {} & -74.47882\,(\mathrm{A}) + 3.04138\,(\mathrm{B}) \\ & + 3.14184\,(\mathrm{C}) + +7.33688\,(\mathrm{D}) \\ & + 744.06483\,(\mathrm{A}^2) \end{aligned} \quad (1)$$

where:
A = Crosslinker (mmol), B = Initiators (mmol), C = Stabilizer (mmol), D = Macromonomer (mmol).
Diagnostic plots show the validity of the model (Fig. 6). The normal probability plot of the residuals is the most important

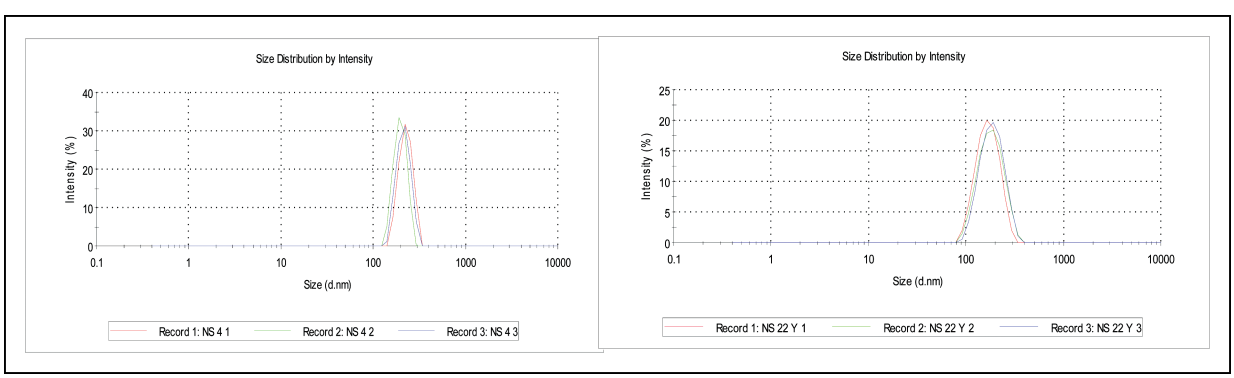

Fig. 4: Typical particle size distribution data of poly-ε-caprolactone nanoparticles prepared by dispersion polymerization.

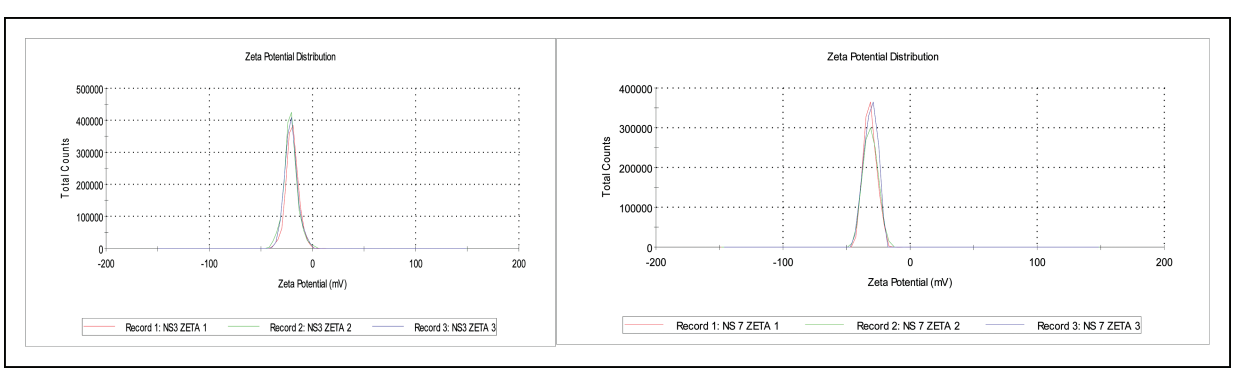

Fig. 5: Typical zeta potential distribution data of poly-ε-caprolactone nanoparticles prepared by dispersion polymerization.

Table 4: Analysis of variance table for particle size

Sum of		Mean	F	p-value		
Source	Squares	df	Square	Value	Prob > F	
Model	1.98	4	0.49	126.80	< 0.0001	significant
Linear Mixture	*1.92*	*3*	*0.64*	*163.82*	*< 0.0001*	
A^2	*0.061*	*1*	*0.061*	*15.71*	*0.0005*	
Residual	0.098	25	3.904E-003			
Lack of Fit	*0.074*	*20*	*3.691E-003*	*0.78*	*0.6921*	*not significant*
Pure Error	*0.024*	*5*	*4.756E-003*			
Cor Total	2.08	29				

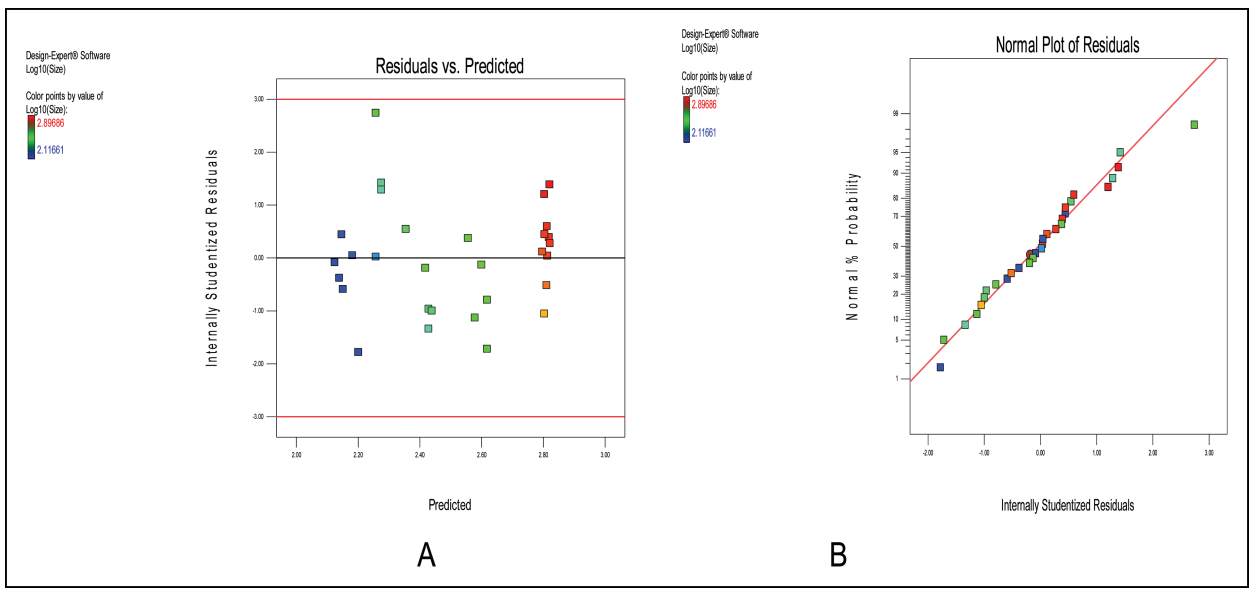

Fig. 6: Typical diagnostic plots for particle size: (A) residuals vs predicted (B) normal plot of residuals.

diagnostic; it checks for non-normality in the error term. A linear normal probability plot of the residuals was obtained which indicates normality in the error term and therefore there is no problem with our data. Further, residuals vs predicted tests the assumption of constant variance and it should be a random scatter within the upper and lower boundaries.

Following square root transformation, model fitting for zeta potential data was carried out. Quadratic model was found significant and the model was selected. To improve the model, insignificant terms were removed by backward elimination. Analysis of variance (ANOVA) (Table 5) reveals that the selected model is significant ($p = 0.0437$). The linear mixture terms (component linear terms) are not significant ($p = 0.7487$); the quadratic term of A (crosslinker) and C (stabilizer) is significant $p = 0.0037$. Also, "lack of fit" is not significant ($p = 0.4389$). Non-significant lack of fit is good; we want the model to fit. Adequate precision measures the signal to noise ratio. The ratio of 6.96 indicates an adequate signal. This model can be used to navigate the design space.

The empirical model (Scheffe polynomial) is shown in Eq. (2) below:

$$\begin{aligned}\text{Sqrt (Negative Surface Zeta Potential} + 0.20) \\ = -644.92273\,(\text{A}) + 24.45442\,(\text{B}) - 32.18851\,(\text{C}) \\ + 12.26659\,(\text{D}) + 2130.94151\,(\text{AC})\end{aligned} \quad (2)$$

Diagnostic plots show the validity of the model (Fig. 7).

2.6. Simultaneous numerical and graphical optimizations of nanoparticle size and nanoparticle surface potential

Following simultaneous numerical optimization of nanoparticle size and nanoparticle surface potential using the two models

Table 5: Analysis of variance table for zeta potential

Source	Sum of Squares	Df	Mean Square	F Value	p-value Prob > F	
Model	43.01	4	10.75	2.87	0.0437	significant
Linear Mixture	*4.58*	3	*1.53*	*0.41*	*0.7487*	*not significant*
AC	*38.43*	*1*	*38.43*	*10.27*	*0.0037*	significant
Residual	93.56	25	3.74			
Lack of Fit	*77.93*	*20*	*3.90*	*1.25*	*0.4389*	*not significant*
Pure Error	*15.63*	*5*	3.13			
Cor Total	136.57	29				

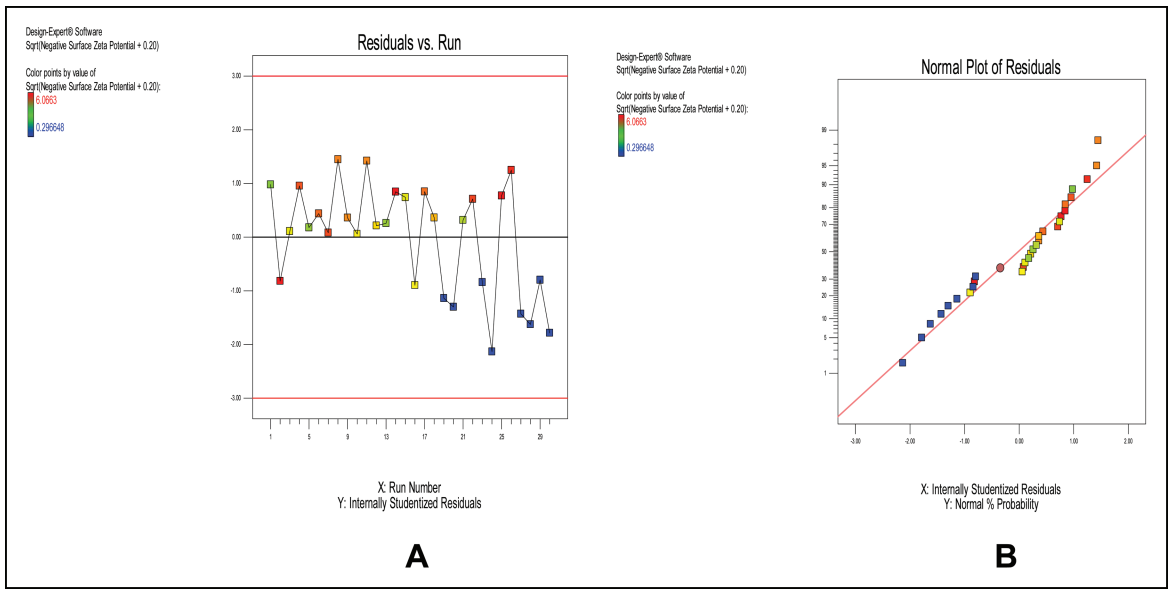

Fig. 7: Typical diagnostic plots for A: residuals vs experimental run (should show a random scatter). B: normal plot of residuals (should give a straight line).

Table 6: Predictability of particle size and zeta potential of poly-ε-caprolactone nanoparticles

Selected Solution	A: Crosslinker (mmol)	B: Initiator (mmol)	C: Stabilizer (PEG-MMA) (mmol)	D: Macromer (mmol)	Predicted Size (nm)	Experimental Size (nm)	Predicted Zeta Potential (mV)	Experimental Zeta Potential (mV)
1	0.035	0.449	0.312	0.204	136.1	121.3	−16.9	−13.1
2	0.036	0.439	0.319	0.207	136.4	128.3	−17.7	−15.0
3	0.030	0.434	0.362	0.174	144.3	152.4	−24.02	−21.5

(Eqs. 1 and 2), ten solutions were returned with desirability values ranging from 0.856 to 0.997 (data not shown). Three of the solutions were used to fabricate nanoparticles to compare the predicted values with the actual laboratory values as shown below (Table 6). The observations from the confirmation experiments are within the confirmation 95% prediction interval (95% PI low and 95% PI high), showing the confirmation of the models (Fig. 8).

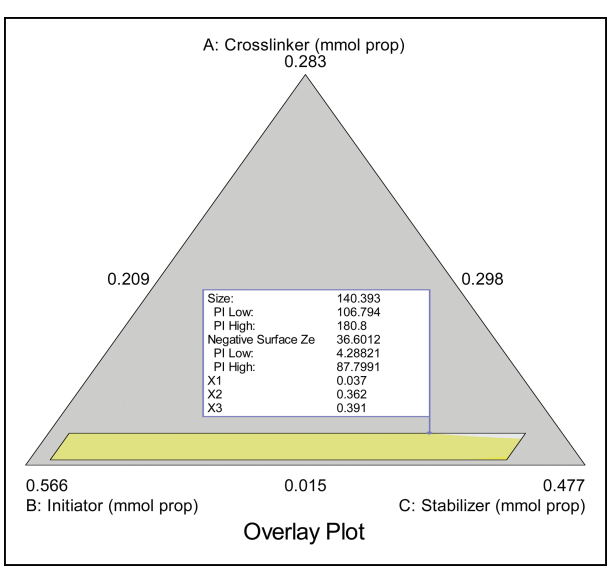

Fig. 8: Overlay plot of particle size and zeta potential with prediction intervals (PI) superimposed on operating window.

The graph shown in Fig. 8 is the overlay plot. The region meeting the specifications for the optimization are colored yellow; it shows the window of operability where the components can be set to meet the requirements for both responses (particle size and surface zeta potential). The flag is planted at the optimum in Fig. 8.

2.7. *In vitro availability*

In vitro release of docetaxel-loaded poly-ε-cparolactone nanoparticles was tested in phosphate buffer saline (PBS) (pH 7.4, IS 0.16). Figure 9 shows the *in vitro* drug release isotherms for two different batches of nanoparticles of different sizes: batch

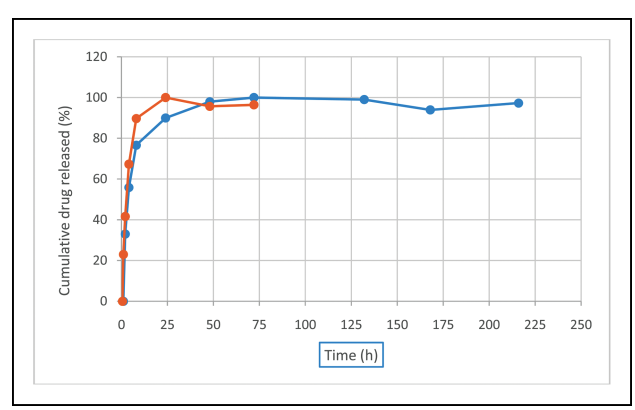

Fig. 9: *In vitro* release isotherms for docetaxel-loaded poly-ε-caprolactone nanoparticles in PBS (pH 7.4, IS 0.16) at 37 °C { = batch 3 Table 6; = batch 1 Table 6} Each point represents the mean value of 3 different experiments (ε 1.37 %; 7.2 %).

1 (121.3 nm) and batch 3 (152.4 nm) (Table 6). The drug loading capacity of poly-ε-caprolactone nanoparticles (batch 1) was 0.8% w/w; while the encapsulation efficiency was 37% w/w. For poly-ε-caprolactone nanoparticles (batch 3), the encapsulation efficiency was 31% while the drug loading capacity was 0.76 % w/w. Drug release was observed over 72 h for batch 3; while batch 1 provided drug release over a period of 120 h. With bigger particle size (Table 6), the release was faster and lasted a shorter time than particles of smaller size (Table 6; Fig. 9). A look at Table 6 shows that the two batches have slightly different amount of crosslinker. The results may reflect the influence of crosslinker: as the crosslinking density decreases, drug release is rapid and lasts a short period. However, care should be taken on this inference because in copolymerization reactions, the amount of crosslinker added may be proportional to but is not equal to the theoretical crosslinking density.
The initial burst release in the two batches can be attributed to docetaxel located just on the surface of the nanoparticles, while the subsequent constant release is primarily as a result of drug diffusion and matrix erosion.

2.8. Conclusion

Stealth biodegradable cross-linked poly-ε-caprolactone nanoparticles were fabricated by free radical dispersion polymerization. The uniqueness of the dispersion polymerization technique is that it is surfactant free, thereby obviating the problems known to be associated with the use of surfactants in the fabrication of nanoparticles for biomedical applications. D-Optimal mixture statistical experimental design was used to generate thirty batches of nanoparticles prepared by varying the proportion of the components (poly-ε-caprolactone macromonomer (synthesized in house), crosslinker, initiators and stabilizer) in acetone/water system. Following simultaneous numerical and graphical optimizations of nanoparticle size and nanoparticle surface zeta potential using the two models generated (Scheffe polynomials), the optimum formulation was identified. *In vitro* availability isotherms show that the nanoparticles sustained the release of docetaxel for 72 to 120 h depending on formulation. The data show that nanotechnology platforms for controlled delivery of bioactive agents can be developed based on the nanoparticles.

3. Experimental

3.1. Materials

ε-Caprolactone was dried over molecular sieves (5 Å) for 48 h and distilled under negative pressure before use. 2-Hydroxyethyl methacrylate (HEMA) (Aldrich, 97%) was dried over molecular sieves (4 Å) for 24 h and distilled under negative pressure before use. Toluene (Acros, 99%) and pyridine (Sigma, ≥ 99%) were refluxed over calcium hydride for one hour and distilled prior to use. Stannous octoate (SnOct) (Sigma, 95%) was used as received. Phosphorus pentoxide (Aldrich, 97%) was also used as received. Hydroxylamine hydrochloride (Sigma, 99%), dichloromethane, and hydrochloric acid (Aldrich, 37%) were used as received. Docetaxel was obtained from Sigma Aldrich and used as received.

3.2. Synthesis of methacrylate-terminated poly-ε-caprolactone macromonomer

ε-Caprolactone (13.14 g), HEMA (3.0 g) and stannous octoate (3 drops) were placed in a 50 mL round bottom flask equipped with a magnetic stir bar. The reaction was kept under vacuum for ten 10 min and polymerization was carried out in an inert atmosphere by flushing the flask with nitrogen gas for 24 h on a silicone oil bath kept at 128°C. The resulting macromonomer was dissolved in dichloromethane (300 mL) and filtered. The macromonomer was precipitated out of this solution using an excess amount of hexane and dry ice. The material was then filtered and dried in a vacuum oven at room temperature under reduced pressure over phosphorus pentoxide for 24 h.

3.3. Synthesis of crosslinking agent (MANHOMA)

The crosslinker was synthesized and characterized based on literature reports (Akala and Okunola 2013; Akala et al. 1998).

3.4. Statistical experimental design

Constraints were introduced to allow the fabrication of nanoparticles on the basis of preliminary experiments. In D-optimal mixture design, there are restrictions on components such that a lower and an upper limits are specified (Adesina et. al. 2013; Shastri et. al. 2013; Rajin 2007; Cornell 2002; Lewis and Chariot 1991) (Table 2). Using these limits, the component amounts of thirty nanoparticle formulations were varied using the Design Expert® statistical software (Stat-Ease Inc., Minneapolis: Wayne and Whitcomb 2014) (Table 3).

3.5. Preparation of blank and drug-loaded crosslinked stealth nanoparticles by dispersion polymerization using redox initiators

A typical preparation of the nanoparticles is as follows: 0.3638 g of poly-caprolactone-HEMA macromonomer, 0.4997 g of polyethylene-glycol methyl-methacrylate (PEG-MMA), with 0.0035 g of crosslinker were dispersed in acetone-water. 0.0805 g of benzoyl peroxide and 0.0605 g of NDPEA (as co-initiators) were injected through the rubber closure under continuous flushing with nitrogen gas and with continuous stirring at 400 rpm. The overall polymerization time was 24 h. The resulting particles were dialysed in dilute hydrochloric acid solution for a period of 24 h and freeze dried to obtain the stealth crosslinked nanoparticles. For drug-loaded particles, the drug was dissolved in the organic layer containing hydrophobic monomers before polymerization and the nanoparticles were recovered by centrifugation. Docetaxel was the prototype drug.

3.6. Characterization of blank and docetaxel-loaded nanoparticles

3.6.1. Particle size and size distribution analysis

Particle size and size distribution of nanoparticles were determined by dynamic light scattering (DLS) using Zetasizer Nano-ZS (Malvern Instruments, USA). 10 mg of freeze-dried particles was redispersed in 5 mL of filtered distilled water using a probe sonicator (Vibra-Cell; Model VC 750, Sonics and Materials, Inc, Newton, CT) at probe amplitude of 30 % for 60 s before measurement. The sonicated suspension was filtered through an acrodisc syringe filter with a 5 μm Versapor membrane (Pall Corporation). Particle size was determined at 25 °C. The mean of three measurements was recorded.

3.6.2. Zeta potential determination

To evaluate the charge on the surface of the particles, the zeta potential was determined using the Zetasizer Nano-ZS (Malvern Instruments, USA) after suspending the particles in PBS at pH 7.4. Three measurements were taken for each sample at 20 °C for 20 s, with an applied voltage of 150 V.

3.6.3. Surface morphology

The surface morphology of the nanoparticles was evaluated using scanning electron microscopy (SEM) (FEI Quanta 200F environmental scanning electron microscope). With this equipment, coating with a metal (e.g. gold) is not necessary and this confers the advantage of imaging accurate morphological features. To evaluate surface morphology, different dilutions of nanoparticle suspension in distilled water were placed on a carbon tape affixed to a specimen stub and dried *in vacuo.* The samples were then viewed using a scanning electron microscope under high vacuum at 10 KV and a working distance of 10 mm. Images were taken at different sample magnifications.

3.6.4. Drug loading and encapsulation efficiency

Drug loading (the weight percent of docetaxel in the nanoparticle formulation) and encapsulation efficiency (percentage of docetaxel that is encapsulated out of the total used for nanoparticle preparation) were determined as follows (Adesina et al. 2013). For encapsulation efficiency (EE) - by quantifying the amount of docetaxel in the dialysis medium (A_{dial}) by high perfomance liquid chromatography (HPLC) and assuming that the rest of the drug used for nanoparticle preparation (A_{prep}) had been encapsulated. The EE was calculated from Eq. (3):

$$EE = \frac{(A_{prep}) - (A_{dial}) \times 100\%}{(A_{prep})} \quad (3)$$

For drug loading (DL) – by dissolving 5 mg of nanoparticles in DMSO (ANP) and quantifying the amount of docetaxel dissolved in the solution

(APIS) by high performance liquid chromatography (HPLC). The percent DL was calculated from Eq. (4):

$$DL = \frac{(APIS) \times 100\%}{(ANP)} \quad (4)$$

3.6.5. In vitro availability studies

Docetaxel-loaded nanoparticles were suspended in phosphate buffered saline (PBS) (pH 7.4; IS 0.16) and placed in a dialysis bag (membrane tubing with molecular weight cut off of 12,000-14,000) in centrifuge tubes containing known volume of PBS and rotated at 360° using a labquake shaker maintained at 37 °C. At specific time intervals, an aliquot of the release medium was taken and replaced with fresh medium each time to continue the release study. The solution was then filtered through a 0.45 μm syringe filter and the amount of docetaxel released into the solution was quantified using a validated HPLC method (high performance liquid chromatography (HPLC) using a HP series 1100 HPLC equipped with a Zorbax 300SB-C18 column kept at 37 °C. The mobile phase for HPLC studies was acetonitrile: water 50% v/v at a flow rate of 1 mL/min. Quantitation of docetaxel was done using Diode Array Detector (DAD) at 230 nm wavelength.

Acknowledgements: The authors wish to thank Dr. John Small, Division Chief, Surface and Microanalysis Science Division, National Institute of Standards and Technology for access to the environmental scanning electron microscope. This work was supported by NCI/NIH Grant #: 1 SC2 CA138179-01, and NIH/NIAID Grant # 5P30A1087714-02 (11-M56R CFDA # 93.855). This work was carried out in facilities supported by NCRR/NIH Grants #1 C06 RR 020608-01 and #1 C06 RR 14469-01.

References

Adesina SK, Wight SA, Akala EO (2013) Optimization of the fabrication of novel stealth PLA-based nanoparticles by dispersion polymerization using D-optimal mixture design. Drug Dev Ind Pharm, in print, doi:10.3109/03639045.2013.838578.

Akala EO, Okunola O (2013) Novel stealth degradable nanoparticles prepared by dispersion polymerization for the delivery of bioactive agents Part I. Pharm Ind 75: 1191–1196; Part II Pharm Ind 75: 1346–1352.

Akala EO, Wiriyacoonkasem P, Pan G. (2011). Studies on *in vitro* availability, degradation, and thermal properties of naltrexone-loaded biodegradable microspheres. Drug Dev Ind Pharm 37: 673–684.

Akala EO (2010) Strategies for transmembrane passage of polymer-based nanostructures. In: Broz P (ed.) Polymer-based nanostructures: medical applications (Royal Society of Chemistry Series 9), Cambridge, UK p.16–80.

Akala EO, Kopeckova P, Kopecek J (1998). Novel pH-sensitive hydrogels with adjustable swelling kinetics. Biomaterials 19: 1037–1047.

Arshady R (1992) Suspension, emulsion, and dispersion polymerization: A methodical survey. Colloid Polym Sci 270: 717–732.

Cafaggi S, Leardi R, Parodi B, Caviglioli G, Bignardi G. (2003). An example of application of a mixture design with constraints to a pharmaceutical formulation. Chemometr Intell Lab Systems 65: 139–147.

Capek I (2000) Surface active properties of polyoxyethylene macromonomers and their role in radical polymerization in disperse systems. Adv. Colloid Interface Sci 88: 295– 357.

Cegnar M, Kos J, Kristl J (2004) Cystatin incorporated in poly(lactide-co-glycolide) nanoparticles:Development and fundamental studies on preservation of its activity. Eur J Pharm Sci 22: 357–364.

Cornell JA (2002) Experiments with Mixtures, 3rd Ed., Wiley, NY.

Couvreur P, Vauthier C (2006) Nanotechnology: Intelligent design to treat complex disease. Pharm Res 23: 1417–1450.

Czelusniak I, Khosravi E, Kenwright AM, Ansell CWG (2007) Synthesis, characterization and hydrolytic degradation of polylactide-functionalized polyoxanorbornenes. Macromolecules 40: 1444–1452.

Dubois PH, Jerome R, Teyssle PH (1991) Macromolecular engineering of polylactones and polylactides. 3. synthesis, characterization, and applications of poly(e-caprolactone) macromonomers. Macromolecules 24: 977–981.

Gillies ER, Fréchet JM (2004) Development of acid-sensitive copolymer micelles for drug delivery. Pure Appl Chem 76:1295–1307.

Ha ST, Park OO, Im SH (2010) Size control of highly monodisperse polystyrene particles by modified dispersion polymerization. Macromol Res 18: 935 – 943.

Han H, Lee J, Hong J, Shim SE (2009) Dispersion polymerization of styrene employing Lyophilic comonomer in the absence of stabilizer: synthesis of impurity-free microspheres. Macromol Res 17: 469–475.

Hillareau H, Couvreur P (2006) Polymeric nanoparticles as drug carriers. In: Uchegbu IF, Schatzlein AG (eds.) Polymers in Drug Delivery, CRC (Taylor & Francis Group), Boca Raton, p.101–110.

Hong J, Hong CK, Shim SE (2007) Synthesis of polystyrene microspheres by dispersion polymerization using poly(vinyl alcohol) as a steric stabilizer in aqueous alcohol media. Colloids Surf A Physicochem Eng Asp 302: 225–233.

Hongliang X, Liangcen C, Gu G, Xiaoqing R, Zhang W, Jieqi L, Yanzuo C, Xinyi J, Xianyi S, Fang Xiaoling F (2010) Enhanced anti-glioblastoma efficacy by PTX-loaded PEGylated poly(ε-caprolactone) nanoparticles: *in vitro* and *in vivo* evaluation. Int J Pharm 402: 238–247.

Horak D (1999) Effect of reaction parameters on the particle size in the dispersion polymerization of 2-hydroxyethyl methacrylate. J Polym Sci A Polym Chem 37: 3785–3792.

Jin C, Wu H, Liu J, Bai L, Guo G (2007). The effect of paclitaxel-loaded nanoparticles with radiation on hypoxic MCF-7 cells. J Clin Pharm Ther 32: 41–44.

Kawaguchi S, Ito K (2005) Dispersion Polymerization. Adv Polym Sci 175: 299 – 328.

Kelkar SS, Reineke TM (2011) Theranostics: combining imaging and therapy. Bioconjugate Chem 22: 1879–1903.

Kim J, Lee C, Jun JB, Suh K (2001) Monodisperse micron-sized crosslinked polystyrene particles. VII. Importance of monomer-diffusible surface characteristics of growing particles. Colloids Surf A Physicochem Eng Asp 194: 57–64.

Kramer-Marek G, Kiesewetter DO, Capala J (2009) Changes in HER2 expression in breast cancer xenograft after therapy can be quantified using PET and 18F-labeled affibody Molecules. J Nucl Med 50: 1131–1139.

Landfester K, Mailander V (2013) Nanocapsules with specific targeting and release properties using miniemulsion polymerization. Expert Opin Drug Deliv 10: 593–609.

Landfester K, Musyanovych A, Mailander V (2010) From polymeric particles to multifunctional nanocapsules for biomedical applications using the miniemulsion process. J Polym Sci Part A 48: 493–515.

Lee K, Lee S, Choi Y, Song B (2004) Dispersion polymerization of acrylamide in t-butyl alcohol/water media. Macromol Res 12: 213–218.

Leobandung W, Ichikaw, H, Fukumori, Y, Peppas NA (2003) Monodisperse nanoparticles of poly(ethylene glycol) macromers and N-isopropyl acrylamide for biomedical applications. J Appl Polym Sci 87: 1678–1684.

Lewis GA, Chariot M (1991) Non classical experimental designs in pharmaceutical formulation.Drug Dev Ind Pharm 17: 1551–1570.

Li S, Huang L (2008) Pharmacokinetics and Biodistribution of Nanoparticles. Mol Pharm 5: 496 – 504.

Liu Y, Schulze M, Albertsson AC (1998) α-Methacryloyl-ω-hydroxyl-poly(ε-caprolactone) macromonomer: synthesis, characterization, and copolymerization J Macromol Sci Pure Appl Chem 35: 207–232.

Oliveira MAM, Boyer C, Nele M, Pinto, JC, Zetterlund PB, Davis TP (2011) Synthesis of biodegradable hydrogel nanoparticles for bioapplications using inverse miniemulsion RAFT polymerization. Macromolecules 44: 7167–7175.

Pitt CG, Gratzl MM, Kimmel GL, Surles J, Schindler A (1981a) Aliphatic polyesters. II. The degradation of poly (dllactide), poly (epsilon-caprolactone), and their copolymers *in vivo*. Biomaterials 2: 215–220.

Pitt CG, Marks TA, Schindler A (1981b) Biodegradable drug delivery systems based on aliphatic polyesters: application to contraceptives and narcotic antagonists. NIDA Res Monogr 28. 232–253.

Rajin M, Bono A, Mun HC (2007). Optimisation of natural ingredient based lipstick formulation by using mixture design. J Appl Sci 7: 2099–2103.

Ray B, Mandal BM (1999) Dispersion polymerization of acrylamide: Part II. 2,2′ azobisisobutyronitrile initiator. J Polym Sci A Polym Chem 37: 493–499.

Reilly RM (2009) Aiming for a Direct Hit: Combining molecular imaging with targeted cancer therapy. J Nucl Med 50:1017–1019.

Ryner M, Finne A, Albertsson Ac, Kricheldorf Hr (2001) L-lactide Macromonomer synthesis initiated by new cyclic tin alkoxides functionalized for brushlike structures. Macromolecules 34: 7281–7287.

Shastri PN, Ubale RV, D'Souza MJ (2013) Implementation of mixture design for formulation of albumin containing enteric-coated spray-dried microparticles. Drug Dev Ind Pharm 39: 164–175.

Schindler A, Jeffcoat R, Kimmel GL, Pitt CG, Wall ME, Zweidinger R (1977) Biodegradable polymers for sustained drug delivery. Contemp Top Polym Sci 2: 251–289.

Shenoy DB, Amiji MM (2005) Poly(ethylene oxide)-modified poly(ε-caprolactone) nanoparticles for targeted delivery of tamoxifen in breast cancer. Int J Pharm 293: 261–270.

Sinha VR, Bansal K, Kaushik R, Kumria R, Trehan A (2004) Poly-epsilon-caprolactone microspheres and nanospheres: an overview. Int J Pharm 278:1–23.

Sinha VR, Khosla L (1998) Bioabsorbable polymers for implantable therapeutic systems. Drug Dev Ind Pharm 24:1129–1138.

Song J, Tronc F, Winnik MA (2006) Monodisperse, controlled micron-size dye-labeled polystyrene particles by two stage dispersion polymerization. Polymer 47: 817–825.

Tortosa K, Miola C, Hamaide T (1997) Synthesis of low molecular weight-hydroxy polycaprolactone macromonomers by coordinated anionic polymerization in protic conditions J Appl Polym Sci 65: 2357–2372.

Ulas AK (2007) A note on model selection in mixture experiments. J Mathem Stat 3: 93–99.

Wayne FA, Whitcomb P (2014). Design Expert Version 9.0.3.1, Stat-Ease, Inc.

Woodward SC, Brewer PS, Moatamed, F, Schindler A, Pitt CG (1985) The intracellular degradation of poly(epsilon caprolactone). J Biomed Mater Res 19:437–444.

Xu P, Van Kirk E, Li S, Murdoch WJ, Ren J, Hussain MD, Radosz M, Shen Y (2006) Highly stable core Surface crosslinked nanoparticles as cisplatin carriers for cancer chemotherapy. Coll Surf B: Biointerfaces 48: 50–57.

Yeon KS, Gyun SI, Moo LY, Su CC, Kiel SY (1998) Methoxy poly(ethylene glycol) and ε caprolactone amphiphilic block copolymeric micelle containing indomethacin. II. Micelle formation and drug release behaviours. J Control Release 51: 13–22.

Yin W, Akala E, Taylor R (2002) Design of naltrexone-loaded hydrolyzable crosslinked nanoparticles. Int J Pharm 244(1–2): 9–19.

Yu LX (2008) Pharmaceutical quality by design: product and process development, understanding, and control. Pharm. Res. 10: 781–791.

Yu LX, Amidon G, Khan MA, Hoag SW, Polli J, Raju GK, Woodcock J (2014) Understanding pharmaceutical quality by design. The AAPS Journal, in print. doi:10.1208/s12248-014r-r9598-3.